LAWRENCE
LIVERMORE
NATIONAL
LABORATORY

UCRL-JRNL-208779

Dynamic response of materials on sub-nanosecond time scales, and beryllium properties for inertial confinement fusion

D. C. Swift, T. E. Tierney, S. N. Luo, D. L. Paisley, G. A. Kyrala, A. Hauer, S. R. Greenfield, A. C. Koskelo, K. J. McClellan, H. E. Lorenzana, M. D. Knudson, P. P. Peralta, E. Loomis

December 28, 2004

Physics of Plasmas

Disclaimer

Dynamic response of materials on sub-nanosecond time scales, and beryllium properties for inertial confinement fusion

Damian C. Swift,* Thomas E. Tierney, Sheng-Nian Luo, Dennis L. Paisley, George A. Kyrala, Allan Hauer, Scott R. Greenfield, Aaron C. Koskelo, and Kenneth J. McClellan
Los Alamos National Laboratory, MS E526, Los Alamos, New Mexico 87545

Hector E. Lorenzana
Lawrence Livermore National Laboratory, 7000 East Avenue, Livermore, California 94550

Marcus D. Knudson
Sandia National Laboratories, Albuquerque, New Mexico

Pedro P. Peralta and Eric Loomis
Arizona State University, Tempe, Arizona 85287
(Dated: November 18, 2004)

During the past few years, substantial progress has been made in developing experimental techniques capable of investigating the response of materials to dynamic loading on nanosecond time scales and shorter, with multiple diagnostics probing different aspects of the behavior. these relatively short time scales are scientifically interesting because plastic flow and phase changes in common materials with simple crystal structures – such as iron – may be suppressed, allowing unusual states to be induced and the dynamics of plasticity and polymorphism to be explored. Loading by laser ablation can be particularly convenient. The TRIDENT laser has been used to impart shocks and isentropic compression waves from ∼1 to 200 GPa in a range of elements and alloys, with diagnostics including surface velocimetry (line-imaging VISAR), surface displacement (framed area imaging), x-ray diffraction (single crystal and polycrystal), ellipsometry, and Raman spectroscopy. A major motivation has been the study of the properties of beryllium under conditions relevant to the fuel capsule in inertial confinement fusion: magnetically-driven shock and isentropic compression shots at Z were used to investigate the equation of state and shock melting characteristics, complemented by laser ablation experiments to investigate plasticity and heterogeneous response. These results will help to constrain acceptable tolerances on manufacturing, and possible loading paths, for inertial fusion ignition experiments at the National Ignition Facility. Laser-based techniques are being developed further for future material dynamics experiments, where it should be possible to obtain high quality data on strength and phase changes up to at least 1 TPa.

PACS numbers:

I. INTRODUCTION

Dynamic loading experiments – usually employing shock waves – are a well-established way of investigating the behavior of materials under extreme conditions of pressure and temperature [1]. Models for many aspects of the response to loading have been motivated by engineering applications, and the fundamental processes have not been established thoroughly and quantitatively. Macroscopic response is governed by the properties of atoms in a crystal (equation of state and elasticity) and the dynamics of defects including dislocations and grain boundaries (plasticity and phase change kinetics), covering a wide range of length scales. Theories and models at each length scale must be tested and validated; experiments probing micrometer and nanosecond time scales are an important component.

Experiments in which dynamic loading is induced with a laser have several inherent benefits for the study of material dynamics. It is relatively easy to synchronize measurements with the drive, so novel diagnostics can be developed and implemented. Samples are often small, making it easier to obtain crystals, and hence to bridge length scales and to investigate hazardous or expensive materials. There is less "collateral" energy and momentum associated with the drive process (compared with, for example, the sabot of a gas gun), making it easier to recover samples for post-shot analysis, with less perturbation to the microstructure. On the other hand, it is difficult to generate a constant pressure by ablation. At higher irradiances, necessary to induce higher pressures, preheating of the material ahead of the loading wave by electrons or x-rays may be significant. Time and length scales of many laser experiments are shorter than for the many shock applications which occur on microsecond time scales, such as loading by the detonation of chemical explosives or the impact of projectiles of millimeter or greater thickness: detailed understanding of physical processes is needed to extrapolate conclusions

*Electronic address: dswift@lanl.gov

from shorter time scales. Further, it can be difficult to obtain adequately prepared and characterized samples of materials of interest.

In short, lasers are a powerful tool to look at physical mechanisms underlying the response of materials to dynamic loading, but they are not the only one. Laser-based experiments are most valuable when used in close conjunction with other experimental techniques (e.g. guns, chemical explosives, magnetic loading, and static presses) and theoretical techniques such as quantum mechanics and molecular dynamics of the atoms in condensed matter.

Here we review recent progress in the use of ablative loading for studies of material dynamics, and diagnostic techniques applied to investigations of the response of materials. We also discuss observations of the behavior of Be under conditions relevant to the fuel capsule for inertial fusion.

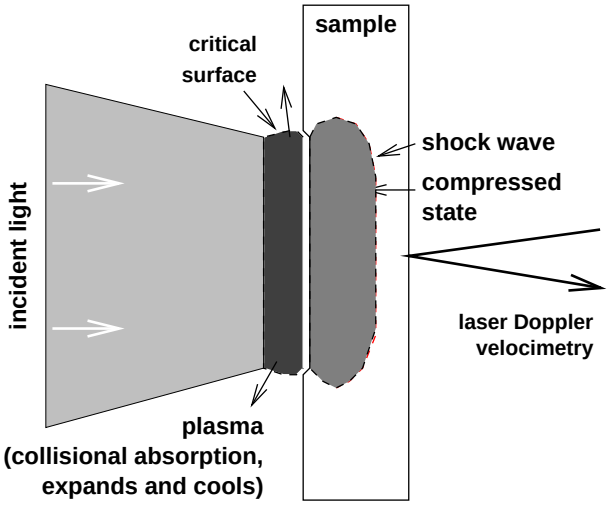

FIG. 1: Schematic of laser ablation experiment for dynamic loading.

II. LOADING BY LASER ABLATION

The work discussed here has focused on dynamic loading induced by ablation of the sample material by a pulse of laser light (Fig. 1), using the TRIDENT laser facility. TRIDENT is based around a flexible three-beam Nd:glass laser with a fundamental wavelength of 1054 nm. For the studies of ablative loading, the laser was operated in nanosecond mode with frequency doubling to 527 nm. In this mode, the laser pulse comprises a stack of 13 elements, each 180 ps long, whose intensity can be controlled essentially independently. Experiments have been performed with an irradiance history designed to produce a shock of constant pressure, a decaying shock (sometimes called a blast wave), or a smooth compression wave. Each of the two main beams could deliver around 200 J, and the third around 40 J. The raw beam from the laser was super-Gaussian in spatial profile; diffractive optical elements were used to distribute the beam uniformly over a circle on the target. These elements produced a flat-top intensity envelope, modulating interference speckles of micrometer scale. Experiments used a 5 mm diameter spot for pressures of up to a few tens of gigapascals, and a 1.5 mm spot for pressures of a few hundred gigapascals.

High-accuracy measurements of states on the Hugoniot of a material require shock waves which have a constant pressure. A constant irradiance does not generally give a constant ablation pressure: the irradiance history must be tailored to induce a constant pressure. In practice, this tailoring can usually be accomplished to only a limited precision. The loading history induced by an arbitrary irradiance history can be predicted with reasonable fidelity using radiation hydrodynamics simulations, and these simulations can be used to adjust material models to improve their accuracy. Procedures for simulating the dynamic loading in this regime have been developed and demonstrated for elements from Be to Au [2]. Models have also been devised for predicting the properties of alloys and compounds in regimes induced in the ablation plasma [3]. However, the loading history is sensitive to transport properties such as the opacity and conductivities, and to numerical parameters in the radiation transport algorithm, as well as to the equation of state (EOS): an error in one model can be compensated by an error in another. Thus we have avoided the use of ablative loading for high-accuracy EOS measurements. We have found no problem in the use of ablative loading to investigate time-dependent phenomena such as plasticity, phase changes, and spall, and to subject samples to variable loading histories, provided the EOS and transport models are adequate for predictions of the loading history induced by the laser pulse.

If laser ablation is used to induce high pressures in a thick sample, the rarefaction following the end of the laser pulse eventually overtakes the leading edge of the compression wave, causing a decay in the peak pressure. For nanosecond-duration pulses, the rarefaction generally catches up in a distance of a few tens of micrometers – the exact value depending on material and drive pressure. Therefore this is the thickness scale to allow the peak pressure to be manifested at the opposite surface, e.g. in a measurement of velocity history, which is the most common diagnostic for investigating gross material response. For a wide range of materials, the flow stress inferred from the elastic wave in the velocity history is much greater on nanosecond-scale experiments than on microsecond scales. Much of the difference is undoubtedly time-dependence in plastic processes, but there may well be a contribution from the texture of the sample, i.e. the precise microstructure of the starting material used in each case. It is relatively uncommon for material of the same microstructure to be used in experiments on both time scales, partly because the crystal size in the larger samples may be too great for representative poly-

crystalline measurements in the smaller samples, partly because the microstructure is not always recorded adequately for subsequent studies, and partly because it can be difficult to cut thin samples without perturbing the microstructure so thin samples are sometimes prepared in other ways e.g. by rolling.

Photons couple predominantly to electrons: during laser ablation, material in the plasma plume reaches thermodynamic equilibrium by electron-ion collisions and interactions with the thermal radiation field, which occur with finite rates. A significant concern in the use of ablative loading is that material ahead of the compression wave may be preheated by non-equilibrium electrons: directly, or indirectly via Bremsstrahlung x-rays. We have never observed any sign of preheating in ablatively-loaded experiments up to at least 100 GPa. Expected signatures in surface velocimetry data, observed with higher irradiances, include motion of the surface before the arrival of the shock and reflectivity changes. Another concern when recovering samples for post-shot analysis is that the hot ablation plasma may cause significant heating of the sample by conduction. Cross-sections of recovered samples of several materials ablatively loaded up to a few tens of gigapascals have shown reproducibly a region $\sim 1\,\mu$m thick of columnar grains strongly suggesting melted and refrozen material, but no other evidence of heating (Fig. 2). Though hot, the ablation plasma has a low density and disperses quickly, so the heat source is only applied to the sample for a short time, and some material is vaporized, reducing the heat conducted. The speckled distribution of the laser induces spatial variations in loading and heating, but these are largely smeared out in the plasma. The ablated surface appears rough in recovered samples, in some cases with surface cracking which may be formed during cooling or refreezing (Fig. 3).

One of the great attractions of laser loading experiments at a flexible facility such as TRIDENT is the capability to change the loading history by altering the irradiance history of the laser pulse. Different regions of thermodynamic space can be explored by using, for instance, a single shock, multiple shocks with release between each, multiple shocks stepping up in pressure, or a smooth compression wave (Fig. 4). Quasi-isentropic compression is of particular current interest, as it explores states relatively far from the Hugoniot measurements which form the primary resource of absolute high pressure states, and in principle a single experiment yields a complete determination of the isentrope up to the peak pressure in the experiment – in contrast to shock experiments which yield a single state per experiment. In isentropic compression experiments (ICE), a smoothly-increasing drive pressure is applied to the sample, and the evolution of the compression wave is monitored as it propagates through different thicknesses of sample; the technique first became popular with magnetic drive [4, 5] but has also been demonstrated with graded-density impactors and by loading the sample with an expanding vapor which may be generated by

FIG. 2: Cross-section of recovered sample, showing columnar grains at the ablated surface. The sample was a single crystal of NiAl. The uniform dark grey area along the left edge is void.

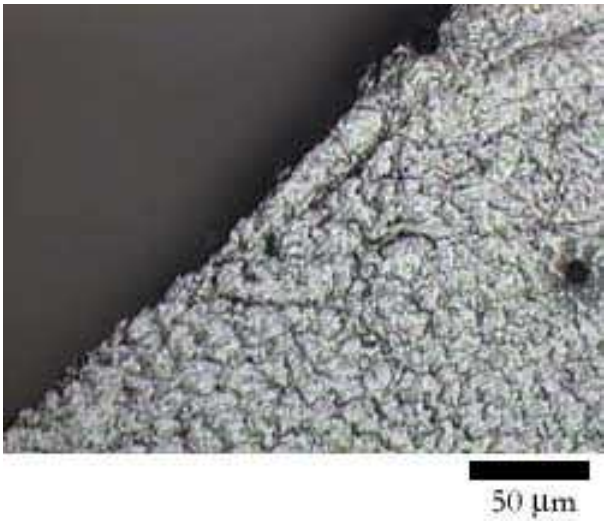

FIG. 3: Ablated surface of recovered sample, showing rough texture with surface cracks. The sample was a single crystal of NiAl.

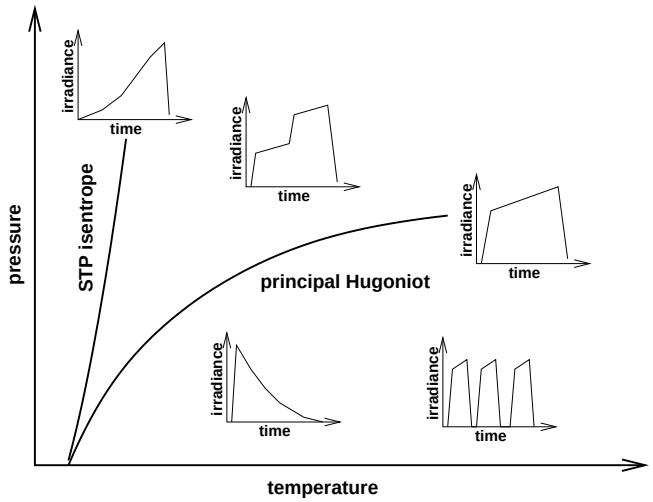

FIG. 4: Regions of state space accessible with different irradiance histories.

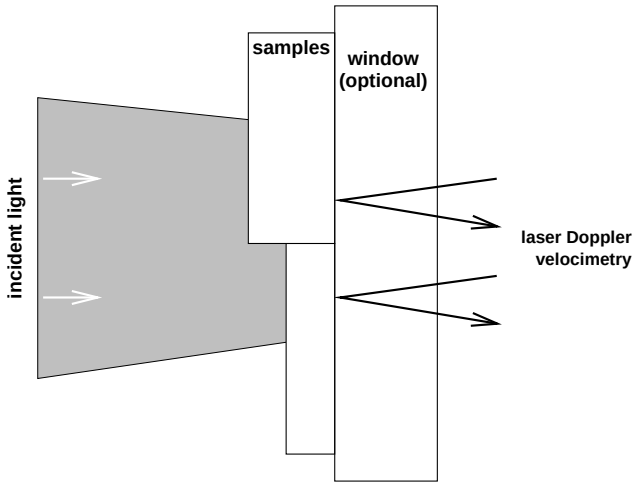

FIG. 5: Schematic of experimental configuration used for laser-driven isentropic compression experiments.

laser heating of a solid [6]. The sample is compressed uniaxially, so plastic flow may occur and heat may be transported by conduction – the loading history may not be perfectly isentropic.

We have demonstrated quasi-isentropic compression using smoothly-ramped ablation pulses [7]. With a nanosecond-scale drive, the useful sample thickness is limited by the distance taken for the compression wave to steepen into a shock. This distance depends on the material and the drive history, in particular the peak pressure. We have performed experiments using samples of different thickness mounted side-by-side and irradiated simultaneously; this approach eliminates uncertainties from shot-to-shot variations in the pulse shape, and the samples can be mounted flush against a window for greater convenience in optical diagnostics (Fig. 5). The response of materials to isentropic compression on nanosecond time scales is potentially extremely interesting, as one would expect some competing deformation mechanisms to be excluded (e.g. slower phase changes, slip systems with a higher Peierls barrier), allowing the remaining mechanisms to be investigated under conditions of higher elastic strain and with less ambiguity in interpretation.

III. DIAGNOSTIC TECHNIQUES

Ablative loading experiments are convenient for developing new experimental diagnostics because synchronization with the optical drive pulse is relatively straightforward. Advanced diagnostics of the material response are also desirable to take advantage of the different regimes of behavior that can be sampled with ablative loading. We have developed and implemented a range of diagnostics at the TRIDENT facility, covering the bulk response of the sample as necessary for developing and testing continuum-level models, and also for exploring the underlying behavior to support the development of physics-based models.

Diagnostics include surface velocimetry and displacement measurements, emission spectrometry, probes of electron-photon and ion-photon interactions, *in-situ* x-ray diffraction, and sample recovery for micrography. Velocimetry can provide data on the EOS, elastic constants, and flow stress. Phase changes can also be deduced through the associated change in volume, compressibility, and strength. Emission spectroscopy is used to determine the surface temperature (usually through a window in order to maintain a finite pressure) and hence the EOS and phase changes. Ellipsometry and Raman spectrometry can be used to constrain the density of phonon states and electron energy levels – components in physics-based EOS – and to indicate phase changes. X-ray diffraction measures the compression – an EOS measurement – and the deformation of the crystal lattice, indicating phase changes and the elastic and plastic strain. Imaging surface velocity and displacement measurements indicate the effect of differently-oriented grains and grain boundaries in a polycrystalline sample.

A. Ellipsometry

Ellipsometry, the polarization-dependence of optical reflectivity, has been used on microsecond-scale experiments as a diagnostic for phase changes in condensed matter [8] and on femtosecond-scale experiments as a diagnostic for laser-matter coupling and condensation in the expanding ablation plume [9]. The polarization-dependent absorption measures the cross-section for electron scattering for different relative orientations of the electric field and the electron wavefunctions; for oblique

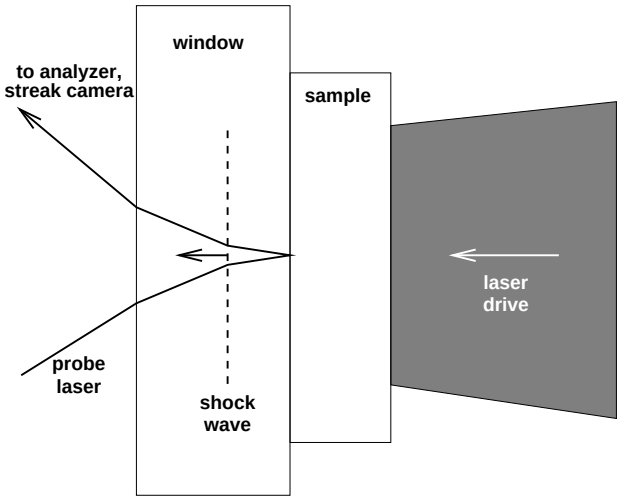

FIG. 6: Schematic of experimental configuration used for ellipsometry measurements.

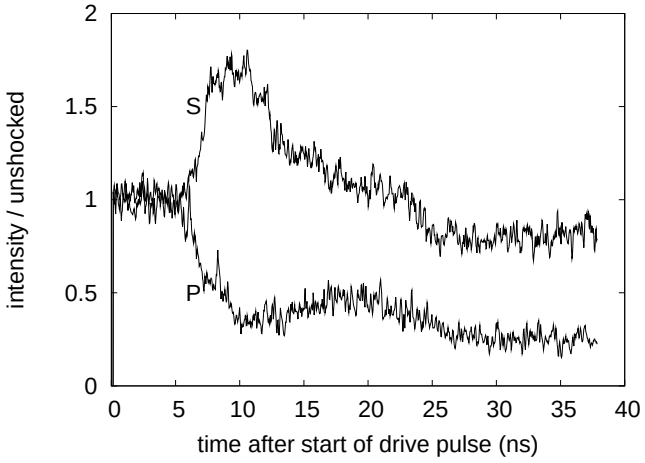

FIG. 7: Ellipsometry signals during shock breakout in Sn. Drive pressure gave 28 GPa on release into the LiF window: sufficient to induce melting. (TRIDENT shot 14972.)

angles of incidence it becomes a measure of the dielectric constant for isotropic materials. These properties generally change if a phase transition occurs, and they also vary with temperature. Using a visible laser source to perform ellipsometry on metals, the measurement only probed a shallow layer at the surface of the sample. Because of concerns about surface effects on the electronic structure and possible surface contamination, we have not so far attempted seriously to relate ellipsometry data to the band structure in a quantitative way, but have investigated its use as an indicator of phase changes.

In the standard TRIDENT material dynamics configuration, ellipsometry measurements were obtained simultaneously with surface velocimetry and emission spectrometry. The sample was clamped against a LiF window to maintain an elevated pressure when the shock reached that surface. The pulsed 660 nm laser used for velocimetry was split and half the light was passed through a depolarizer and directed to a point on the surface at an angle $\sim 20°$ to the normal. Specularly-reflected light was relayed to a polarizing beamsplitter cube, and the resulting signals for two orthogonal polarizations recorded on a streak camera. The polarizing cube was oriented to measure polarizations parallel to the surface and normal to that direction (P and S). (Fig. 6.)

Experiments were performed with high-purity Sn samples. Sn has a higher shock impedance than LiF at pressures of a few tens of GPa, so the state at the window interface had a lower pressure than behind the shock in the bulk material. At a pressure sufficient for the Sn to melt on release into the LiF, the relative intensities of S and P polarized light changed rapidly when the shock reached the Sn/LiF interface (Fig. 7). At lower pressures, no change was observed in the relative intensities. A series of experiments was performed using W samples, to investigate whether the changing ellipsometry signal could be caused by the response of the LiF rather than the Sn; at pressures up to at least $\sim$200 GPa, no measurable change was observed in the ellipsometry signal.

B. Polycrystal diffraction

We have previously obtained in-situ x-ray diffraction signals during shock loading of single-crystal samples. X-rays were produced by focusing a second beam of the TRIDENT laser to a spot $\sim 100\,\mu$m in diameter on a metal foil, $\sim 10\,\mu$m thick, to induce a plasma which cooled by emitting predominantly He-like line radiation. In the single-crystal experiments, the foil was positioned 10 to 15 mm from the sample. The angle of incidence of the x-rays varied with position across the surface of the sample, and where the Bragg condition was satisfied a line was diffracted. As the crystal lattice parameters varied during loading, diffraction occurred at different positions over the surface, and the changing origin and angle were recorded with time-integrating film and time-resolving x-ray streak cameras [10].

Because the diffracting point moves with compression, there is a limit to the range of compressions which can be measured on a single experiment. This is a drawback for experiments on Be, as melt occurs at pressures of 150 to 200 GPa, requiring a high compression and thus a small drive spot of around 1 mm diameter at TRIDENT. It is desirable to compare Be with Be-Cu alloy, but it may not be possible to obtain alloy of suitable composition in single-crystal form, and it is desirable in any case to investigate melting in material with a relevant microstructure. Further, if a material undergoes a solid-solid phase change, the daughter phase may be polycrystalline even if the original sample was a single crystal. Be transforms from hexagonal to body-centered cubic before melting at

ambient pressure; this transformation may occur under dynamic loading.

We have developed techniques for collecting diffraction data over a wider range of Bragg angles, with large-area x-ray detectors and by moving the x-ray source closer to the sample. We have also investigated diffraction from polycrystalline samples. In the initial experiments, the x-ray source was in the same place as for the single-crystal experiments, but a collimator was added between the source and the sample, to sample diffraction from one small spot on the sample surface (Fig. 8). The collimator was an Al disk with a hole drilled along the axis; the disk could be tilted to change the size of the x-ray spot on the surface of the sample. The samples were rolled foils of Be 55 μm thick; the orientation of the c-axis in each grain was far from isotropic, but was distributed over a range of a few tens of degrees from the foil normal. Other crystal axes were distributed more isotropically in the plane of the sample. With a Be sample and a Ti x-ray source, the resulting 4.61 Å x-rays were attenuated little through the sample, so the diffraction signal was integrated through the full thickness of the sample, i.e. over any compressions present. The relative orientation of the source, sample, and detector were set so that the reflection from (0002) planes should be in the center of the field of view. With no shock induced in the sample, a diffraction arc was observed on the time-integrating film, and its thickness decreased if the collimator was tilted, ultimately leaving the doublet structure characteristic of the source spectrum. With an ablation-induced shock wave of the order of 10 GPa, lines were also seen from compressed material, most clearly on the more sensitive x-ray streak record. Comparing with radiation hydrodynamics simulations and analysis of surface velocity histories, the x-ray record can be interpreted as a superposition of uniaxial crystal strain in the elastic wave and isotropic strain in the plastic wave. The compressed diffraction signal spanned a range consistent with strains in these two modes of deformation. (Fig. 9.)

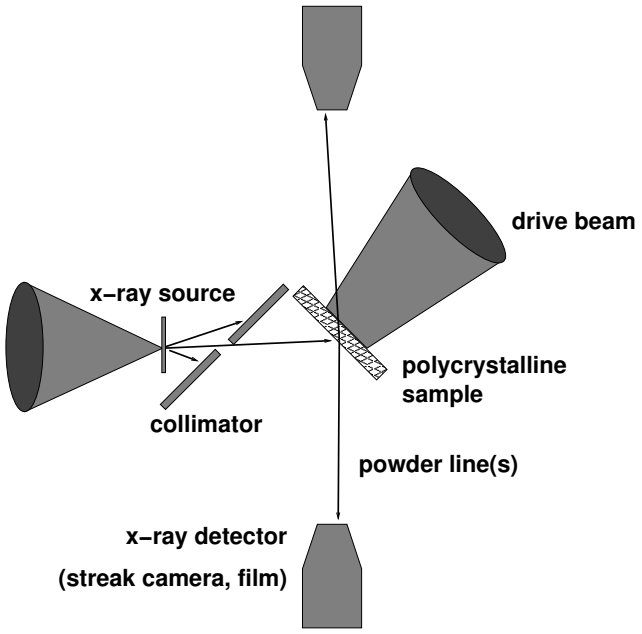

FIG. 8: Schematic of experimental configuration used for diffraction measurements from polycrystalline samples.

C. Imaging displacement interferometry

By using the surface of the sample as in one arm of an imaging Michelson interferometer, spatial variations in surface displacement can be measured as a function of time during a shock wave experiment, to investigate the effect of differently-oriented grains and grain boundaries on the behavior of material under dynamic loading. Time resolution was obtained by operating the interferometer with a comb of 527 nm pulses 180 ps long and 6 ns apart, from the TRIDENT front end, with the interference pattern recorded using an 8-image framing camera with a 5 ns exposure time per independently-timed frame. The ablative drive also used this wavelength, but at $\sim$200 μm, the samples were sufficiently thick that any stray light from the drive beam had dissipated before the first frame in the displacement sequence. In this way, images were obtained simultaneously with line-imaging surface velocimetry, with a displacement resolution $\sim$10 nm and a spatial resolution $\sim$20 μm, with considerable scope for improvement. Experiments have been performed on NiAl bicrystals, Si crystals, and Cu foils. The different crystal orientations in NiAl, which is anisotropic, led to clearly measurable differences in displacement history and to surface waves originating at the grain boundary (Fig. 10).

IV. BERYLLIUM PROPERTIES FOR THE INERTIAL FUSION CAPSULE

Ignorance about the properties of Be in the inertial confinementt fusion (ICF) capsule regime include the pressure required to melt it under dynamic loading and its orientation-dependent flow stress on nanosecond time scales. The thermal EOS has not been measured at high pressures, so the equilibrium melting curve cannot be estimated with certainty using the Lindemann law. Different published EOS [11, 12] for Be have very different loci for the principal Hugoniot in pressure-temperature space. Further, there is evidence that the melting transition may exhibit significant time-dependence on time scales of a microsecond and shorter [13], which can be treated as a superpressurization necessary to induce catastrophic melting, i.e. to a melting curve displaced to higher pressures. (Fig. 11.)

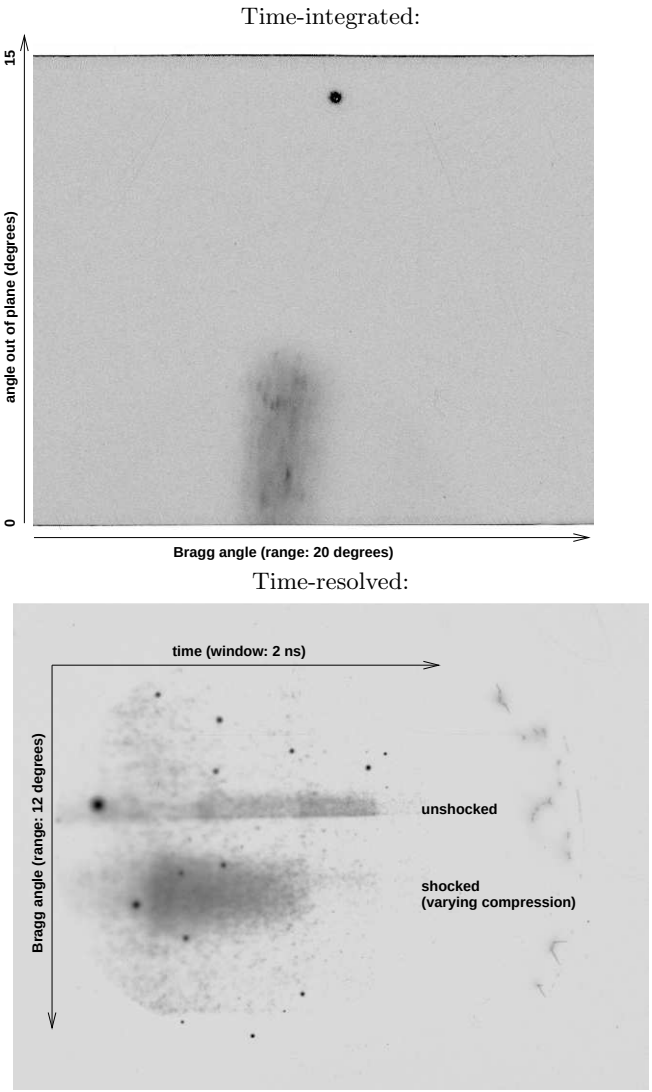

FIG. 9: Example results from polycrystalline diffraction experiment on a rolled Be foil 55 μm thick. Drive pressure was 11 ± 1 GPa. Broad diffraction line spans a range equivalent to 7.1 to 18.4 GPa in isotropic strain, or 3.4 to 8.1 GPa in uniaxial strain. The flow stress in Be foils deduced from velocimetry was ∼2.5 to 6 GPa.

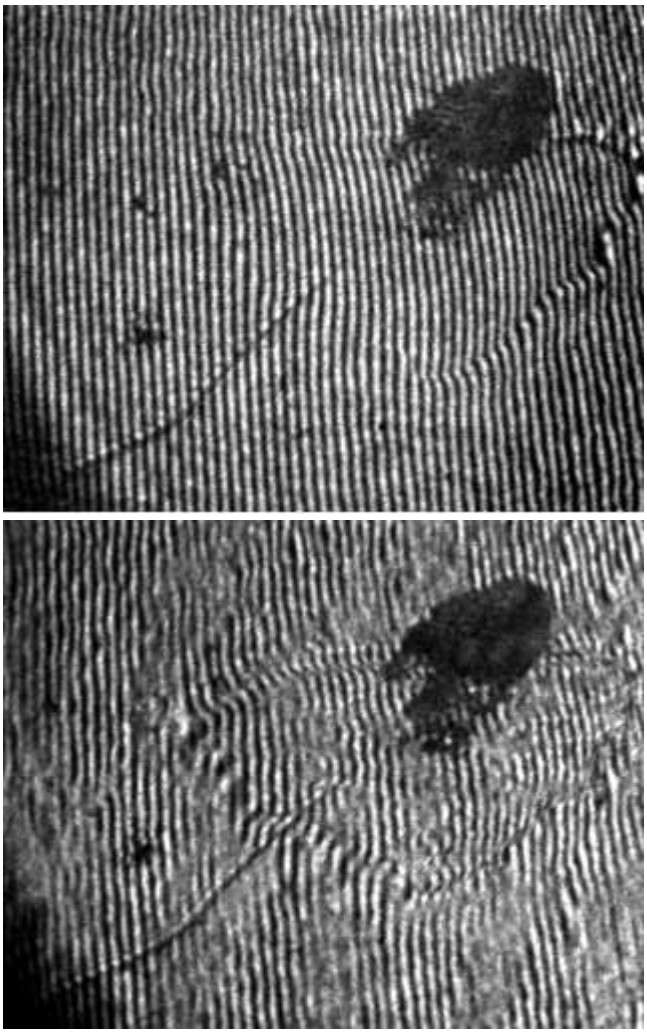

FIG. 10: Example experimental data from imaging displacement interferometer: NiAl bicrystal, 1×1 mm field of view, frames at 6 ns intervals after shock breakout. Large black blob is an ink alignment mark. If surface was flat, fringes would be straight and uniform. Included crystal near the center can be seen from its relative displacement; surface waves are also visible originating at the grain boundary.

A. Equation of state and melting

Experiments were performed at the Z facility to measure the mechanical EOS of Be along different loading paths: the principal Hugoniot and isentrope, up to pressures ∼200 GPa appropriate to the foot of the NIF laser drive. The square or rectangular short configuration was used to induce magnetic loading in the conductor from the pulsed power discharge. This loading was then used to accelerate flyer plates for impact-induced shocks or to drive a smooth compression wave for isentropic compression.

In the Hugoniot experiments, the flyer impacted a target stack in which the Be sample was sandwiched against a LiF window. The velocity history at the Be/LiF interface was measured by laser Doppler velocimetry (point VISAR [14]). Shock states were deduced from the flyer speed on impact and either the shock transit time or the peak particle velocity in the shock. There was some difficulty in identifying the instant of impact, so the states deduced with least uncertainty used the particle velocity. These Hugoniot states agreed well with predictions from published EOS for Be, filling in a gap in the experimental data between gas gun and nuclear impedance mismatch data. Comparing the measured velocity histories with continuum mechanics predictions using the measured flyer speed, several detailed aspects of the ex-

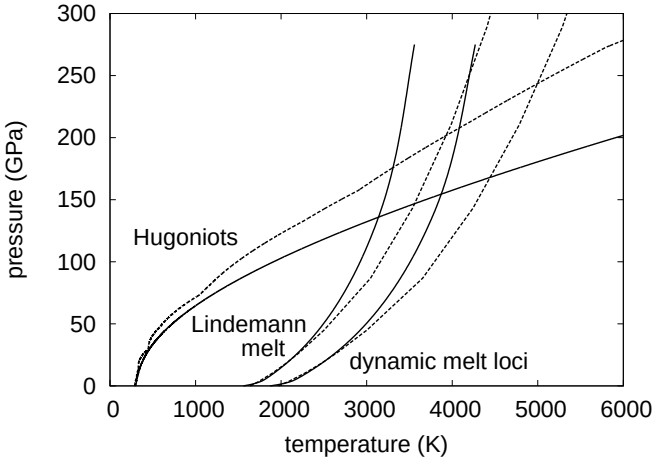

FIG. 11: Phase diagram of Be, showing principal Hugoniot, Lindemann melt curve, and effective melt locus under nanosecond-scale loading, predicted using SESAME (solid) and Steinberg (dashed) equations of state.

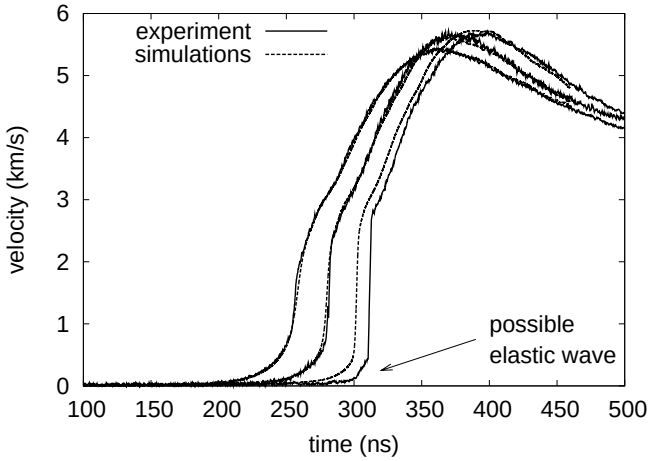

FIG. 12: Velocity history for different thicknesses of Be sample during isentropic loading: experiment and simulations using different equations of state.

periments – such as residual conductor material on the back of the flyer – had to be added to match features in the data. A few features remained unaccounted-for: these are possible signals of melt under dynamic loading. The corresponding candidate melt states can only be associated with a temperature by assuming an EOS, so they are not a unique determination of shock melting.

The different EOS predicted somewhat different loci for the principal isentrope, even in mechanical parameters. The quasi-isentropic compression experiments were performed to see whether this difference could be used to identify which EOS was likely to be most accurate for temperature. The pulsed power discharge was used to drive a compression wave into Be samples of different thickness mounted on the Al conductor: zero (Al only), 250 μm and 500 μm. In each case the velocity history was measured for the surface in contact with a LiF window. The design current history was used to predict the nominal loading history; this was refined iteratively to reproduce the velocity history at the Al/LiF interface, and thus to predict the velocity history at the Be/LiF interfaces for each EOS. The velocity histories for the different EOS were substantially in agreement, and matched the experimental trace for the 250 μm sample to within its error: this isentropic compression experiment could not discriminate between the different EOS (Fig. 12). The experimental record for the 500 μm sample was significantly different from the simulations though nominally exploring the same isentrope: there may have been a gap in the assembly.

B. Plasticity

Ablative loading experiments were performed at TRIDENT to investigate the plasticity in Be under dynamic loading, principally using laser Doppler velocimetry measurements (line-imaging VISAR) of the elastic wave and plastic shock. Experiments were performed with single crystals, cut parallel to (0001) planes, and with rolled foils. The samples were around 30 μm thick. X-ray diffraction data were obtained simultaneously with velocimetry for the crystals [15] and reinforced the interpretation of the velocity data.

On nanosecond time scales, the flow stress in Be was found to be high – the elastic wave had a large amplitude – and the detailed plastic response was sensitive to the microstructure: the shape of the precursor was significantly different for the crystal compared to the rolled foil. In the crystal, the elastic wave rose more quickly than the VISAR could resolve, then the surface decelerated slightly ahead of the plastic shock; in contrast, the elastic wave in the foil rose more slowly to a lower value (Fig. 13). Performing continuum mechanics simulations with time-independent strength models, parameters calibrated to microsecond-scale experiments [12] underpredicted the amplitude of the precursor by an order of magnitude. Adjusting the flow stress, the amplitude of the initial peak could be reproduced, but not the subsequent profile (Fig. 14). Using a time-dependent plasticity model calibrated to microsecond-scale experiments – the Steinberg-Lund model [12] – no plastic flow was predicted: this model apparently overpredicted the sensitivity to time scale.

An orientation-dependent strength model is needed in any case for simulations of loading in polycrystalline capsules, so the single-crystal data were interpreted in the context of microstructural contributions to plasticity. In

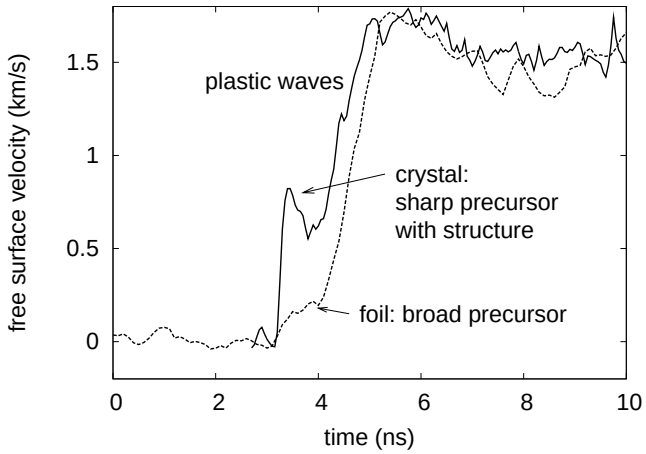

FIG. 13: Free surface velocity history for Be: (0001) crystal compared with rolled foil.

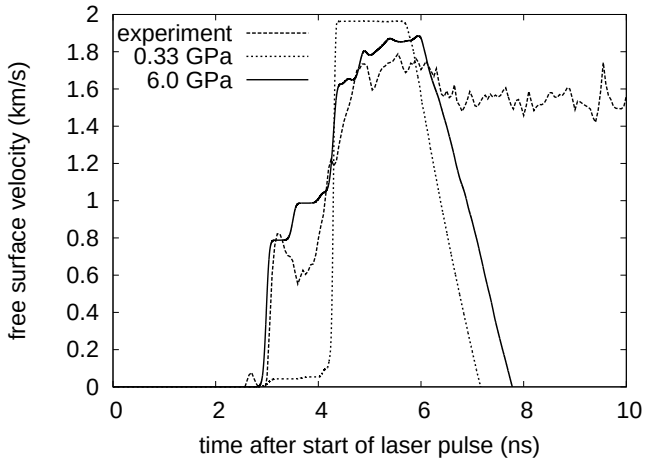

FIG. 14: Free surface velocity history for Be (0001) crystal: experiment compared with elastic-plastic model using microsecond-derived parameters (low amplitude) and flow stress adjusted to match initial peak in the experiment.

the present work, this was not a complete crystal plasticity model, but a single term characteristic of one deformation mode. At the microstructural level, plasticity proceeds by the motion of line or area defects: dislocations or twin boundaries. As they move, the mean plastic strain changes so as to reduce the elastic strain energy. The potential experienced by an atom or defect is proportional to $\sin^2(\pi\epsilon/b)$, where ϵ is the linear displacement and b the length of the Burger's vector for slip in the crystal lattice. At the most simple level, motion by the defect occurs as an Arrhenius-like hopping process with thermal activation over an energy barrier. Thermally-activated hopping can occur in principle in the direction of increasing or decreasing elastic strain. In this model, the forward and reverse rates are biased by a term in the

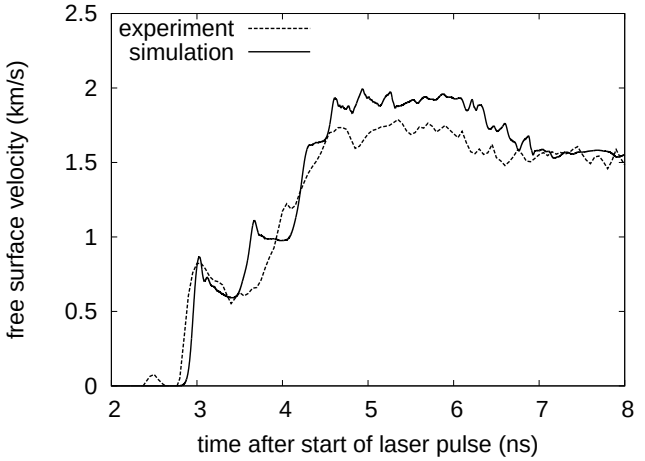

FIG. 15: Free surface velocity history for Be (0001) crystal: ablative loading experiment compared with microstructural plasticity model. Simulation used a spall stress of 2 GPa.

current elastic strain which decreases the barrier for hopping to decrease elastic strain and increases the barrier for hopping to increase elastic strain:

$$\dot{\epsilon}_p = \alpha(\rho)\left\{\exp[-T^*(1-\gamma)/T] - \exp[-T^*(1+\gamma)/T]\right\} \tag{1}$$

where

$$\gamma(\epsilon_e) \equiv \sin^2\left(\frac{\pi\epsilon_e}{b(\rho)}\right). \tag{2}$$

The activation temperature T^* was calculated from the Peierls barrier: 3600 K [12] – a microstructural parameter. Good fit to initial peak and deceleration was obtained for a hopping attempt rate $\alpha = 2000$/ns: a reasonable number for atomic vibrations (Fig. 15).

A more general model is under development describing the plastic strain rate for each slip system. Further experiments on single crystals – particularly other orientations – are highly desirable to calibrate the model, though some calibration will be performed using molecular dynamics simulations. When complete, the plasticity model will be used in simulations of the effect of NIF-like loading on representative resolved microstructures, to predict the velocity spectrum as a function of position and time. Perturbations to the mean velocity can be equated to an equivalent surface roughness in their seeding of ablative Rayleigh-Taylor instabilities, allowing a microstructure specification to be made for ICF capsule material [16].

V. PROSPECTIVE FOR EXPERIMENTS AT THE NATIONAL IGNITION FACILITY

Many of the techniques developed and measurements performed were intended to support projects at the National Ignition Facility (NIF) in one form or another:

techniques which could be used in NIF experiments and characterization of material planned to be used in ignition experiments. The energy, beam orientations, and pulse shaping at the NIF offer the prospect of highly advanced experiments exploring extreme material states in unprecedented detail. The main concern is that the new experimental platforms needed to reach these states may be more prone to pathological laser-related problems such as preheating, where they have not perturbed measurements at lower pressures. Some initial platforms are under development, such as high-temperature hohlraums, long-pulse hohlraums, and the vapor-driven scheme for isentropic compression [6], using supporting experiments (scaled or lower pressure) at other facilities such as the OMEGA laser. However, the amount of energy available at the NIF is so large compared with previous laser systems that, for material dynamics experiments, there is likely to be a significant advantage in using other strategies to investigate states in which the full energy in hohlraum or laser ablation is not needed. For example, it seems possible to apply the energy over a much larger volume – possible with confined ablation, as used in previous flyer launch and shock experiments [17, 18], and inducing a modest drive pressure of ∼1 to 100 GPa, in the range demonstrated to avoid preheat – and taking advantage of shock dynamic effects such as convergence and Mach reflection to increase the pressure, as has been done with chemical explosives [1]. Laser-based equivalents of this approach are under development.

VI. CONCLUSIONS

We have demonstrated the versatility of ablative loading with temporally-shaped laser pulses at TRIDENT. It is practicable to perform experiments with a sustained shock, multiple shocks, a decaying shock, or a smooth compression wave by relatively straightforward adjustment of the pulse shape, the rest of the experiment (target and diagnostics) remaining essentially unchanged. Diagnostics were developed and fielded which can be used to measure the EOS, flow stress, phase changes, heterogeneous response, and electronic and lattice processes. The diagnostics include imaging surface velocity and displacement, emission and reflection spectrometry, and x-ray diffraction.

The dynamic plasticity of Be was investigated on nanosecond time scales with ablative loading. The plastic response was significantly different than would be predicted using existing models developed to fit microsecond-scale experiments, but was consistent with a model representing microstructural processes. Published EOS reproduced mechanical data on the principal Hugoniot and isentrope of Be to ∼200 GPa. These experiments did not discriminate between alternative EOS, and thus between the quite different temperatures predicted on the Hugoniot. More work is needed to predict shock melting conditions for Be: in-situ temperature and structure measurements are highly desirable.

The outlook for experiments at the NIF is very promising: it should be possible to prepare matter in more extreme thermodynamic states than previously accessible to experimenters, and to probe these states accurately and with new diagnostics.

VII. ACKNOWLEDGMENTS

We would like to acknowledge the contributions of many individuals and teams to aspects of the work reported in this paper. The staff of TRIDENT and Z were essential in the successful performance of the experiments. Jason Cooley, Dan Thoma, Ken McClellan, Darrin Byler, Ron Perea, Bob Springer, John Bingert, Bob Day, and Art Nobile of the Materials Science and Technology Division were involved in preparing samples and targets. The pulse shaping relied heavily on the efforts of Randy Johnson. Roger Kopp, Paul Bradley, Doug Wilson, and Nels Hoffman of the Applied Physics Division provided advice and support for radiation hydrodynamics simulations. Doran Greening, also of Applied Physics, was involved in developing microstructural plasticity models.

Funding and project support were provided by Allan Hauer, Nels Hoffman, Cris Barnes, and Steve Batha (Thermonuclear Experiments); Aaron Koskelo (Chemistry Division) who was Principal Investigator of the Laboratory-Directed Research and Development project entitled 'New Windows into Shocks at the Mesoscale;' and Bruce Remington (Lawrence Livermore National Laboratory) via his NIF Materials Integrated Experimental Team. This work was performed under the auspices of the U.S. Department of Energy under contract # W-7405-ENG-36 and W-7405-Eng-48 with UC, LLNL.

[1] A.V. Bushman, G.I. Kanel', A.L. Ni, and V.E. Fortov, *Intense Dynamic Loading of Condensed Matter* (Taylor and Francis, London, 1993).
[2] D.C. Swift, T.E. Tierney IV, R.A. Kopp, and J.T. Gammel, Phys. Rev. E **69**, 036406 (2004).
[3] D.C. Swift, J.T. Gammel, and S.M. Clegg, Phys. Rev. E **69**, 056401 (2004).
[4] J.R. Asay, in *Shock Compression of Condensed Matter – 1999*, edited by M.D. Furnish, L.C. Chhabildas, and R.S. Hixson (American Institute of Physics, New York, 2000), p. 261.
[5] D.B. Reisman et al, J. Appl. Phys. **89**, 1625 (2001).
[6] J. Edwards et al, Phys. Rev. Lett. **92**, 075002 (2004).
[7] D.C. Swift and R.P. Johnson, *Quasi-isentropic compression by ablative laser loading: response of materials to dynamic loading on nanosecond time scales*, submitted

to Phys. Rev. E (2004).
[8] J. Nguyen (Lawrence Livermore National Laboratory), private communication (2002).
[9] H. Yoneda, H. Morikami, K. Ueda, and R.M. More, Phys. Rev. Lett. **91**, 7, 075004/1-4 (2003).
[10] D.C. Swift, G.J. Ackland, A. Hauer, and G.A. Kyrala, Phys. Rev. B **64**, 21, 214107 (2001).
[11] S.P. Lyon and J.D. Johnson (Los Alamos National Laboratory), *SESAME: the Los Alamos National Laboratory equation of state database*, Los Alamos National Laboratory report LA-UR-92-3407 (1992).
[12] D.J. Steinberg, *Equation of state and strength properties of selected materials*, Lawrence Livermore National Laboratory report UCRL-MA-106439 change 1 (1996).
[13] S.-N. Luo, T.J. Ahrens, T. Cagin, A. Strachan, W.A. Goddard III, and D.C. Swift, Phys. Rev. E **68**, 134206 (2003).
[14] L.M. Barker and R.E. Hollenbach, J. Appl. Phys. **43**, 4669 (1972).
[15] D.C. Swift, D.L. Paisley, G.A. Kyrala, and A. Hauer, in *Shock Compression of Condensed Matter – 2001*, edited by M.D. Furnish, N.N. Thadhani, and Y. Horie (American Institute of Physics, New York, 2002), p. 1192.
[16] N.M. Hoffman and D.C. Swift, in *Shock Compression of Condensed Matter – 2003*, edited by M.D. Furnish, Y.M. Gupta, and J.W. Forbes (American Institute of Physics, New York, 2004), p. 1339.
[17] D.C. Swift, J.G. Niemczura, D.L. Paisley, R.P. Johnson, S.-N. Luo, and T.E. Tierney, *Laser-launched flyer plates for shock physics experiments*, submitted to Rev. Sci. Instrum. (2004).
[18] J. Colvin (Lawrence Livermore National Laboratory), private communication (2002).